MOLECULAR AND CELLULAR BIOLOGY, May 2003, p. 3067–3078 Vol. 23, No. 9
0270-7306/03/$08.00+0 DOI: 10.1128/MCB.23.9.3067–3078.2003


# Autoinhibition of the Kit Receptor Tyrosine Kinase by the Cytosolic Juxtamembrane Region

Perry M. Chan,[1]† Subburaj Ilangumaran,[1] Jose La Rose,[1] Avijit Chakrabartty,[2] and Robert Rottapel[1,2,3,4]*

*Division of Experimental Therapeutics, Ontario Cancer Institute, Princess Margaret Hospital, Toronto, Ontario M5G 2M9,[1] Department of Medical Biophysics[2] and Departments of Immunology and Medicine,[3] University of Toronto, Toronto, Ontario M5S 1A8, and St. Michael's Hospital, Toronto, Ontario M5B 1W8,[4] Canada*

Received 24 June 2002/Returned for modification 8 August 2002/Accepted 27 January 2003

**Genetic studies have implicated the cytosolic juxtamembrane region of the Kit receptor tyrosine kinase as an autoinhibitory regulatory domain. Mutations in the juxtamembrane domain are associated with cancers, such as gastrointestinal stromal tumors and mastocytosis, and result in constitutive activation of Kit. Here we elucidate the biochemical mechanism of this regulation. A synthetic peptide encompassing the juxtamembrane region demonstrates cooperative thermal denaturation, suggesting that it folds as an autonomous domain. The juxtamembrane peptide directly interacted with the N-terminal ATP-binding lobe of the kinase domain. A mutation in the juxtamembrane region corresponding to an oncogenic form of Kit or a tyrosine-phosphorylated form of the juxtamembrane peptide disrupted the stability of this domain and its interaction with the N-terminal kinase lobe. Kinetic analysis of the Kit kinase harboring oncogenic mutations in the juxtamembrane region displayed faster activation times than the wild-type kinase. Addition of exogenous wild-type juxtamembrane peptide to active forms of Kit inhibited its kinase activity in *trans*, whereas the mutant peptide and a phosphorylated form of the wild-type peptide were less effective inhibitors. Lastly, expression of the Kit juxtamembrane peptide in cells which harbor an oncogenic form of Kit inhibited cell growth in a Kit-specific manner. Together, these results show the Kit kinase is autoinhibited through an intramolecular interaction with the juxtamembrane domain, and tyrosine phosphorylation and oncogenic mutations relieved the regulatory function of the juxtamembrane domain.**

Receptor tyrosine kinases (RTKs) activate intracellular signaling pathways that control cellular growth, differentiation, and metabolism. The catalytic activity of RTKs is tightly controlled through a number of mechanisms, including ligand binding, internalization and degradation, and the activation of protein tyrosine phosphatases (14, 37). Disruption of any of these control points can lead to constitutive receptor activation and subsequent cellular transformation.

Recently, mutations in Kit which result in ligand-independent activation of the kinase were found to be associated with human gastrointestinal stromal tumors (GISTs) (15) and mastocytosis (11). Kit mutations in GISTs most frequently occur in the noncatalytic juxtamembrane (JM) region, suggesting that this region is crucial in regulation of kinase activity (28). GIST JM mutations are comprised of deletions, substitutions, a combination of deletions and substitutions, or tandem duplications. The retroviral version of Kit originally identified in a feline sarcoma retroviral complex also has mutations and deletions in the JM region (3).

Two other members of the type III RTK family, platelet-derived growth factor receptor β (PDGFRβ) and Flt3, have been reported to contain activating mutations in their JM regions (13, 19, 29, 32). Similar to Kit, these mutations result in ligand-independent kinase activation. The Flt3 JM mutations are tandem duplications and occur in approximately 20% of acute myeloid leukemia patients, making Flt3 the most mutated protein of human acute myeloid leukemia. Other RTKs reported to be regulated by the cytosolic JM region include the vascular endothelial growth factor receptor 1 (12) and the ephrin B4 receptor (4). Together, these observations point to a general function of the JM region as a negative regulator of RTK catalytic activity.

Here we investigated the role of the Kit JM region in regulating the activity of the kinase domain. We showed that the JM region comprises a cooperatively folded domain that bound to the N-terminal ATP-coordinating lobe of the kinase domain. An oncogenic mutation in the JM domain resulted in decreased stability and lowered affinity for the N-terminal lobe. Similarly, tyrosine phosphorylation of the Kit JM region resulted in disruption of its secondary structure and diminished binding to the N-terminal lobe of the kinase. The induction time for Kit activation was dramatically decreased when the JM region was deleted or mutated. Addition of exogenous wild-type JM peptide to active forms of Kit inhibited its phosphotransferase activity in *trans*, whereas the mutant and the tyrosine-phosphorylated peptide were less effective inhibitors. Lastly, overexpression of the Kit JM peptide in cells transformed by an oncogenic form of Kit could suppress the growth characteristics of those cells in a Kit-specific manner. We propose a model of Kit kinase regulation in which the JM region functions as an autonomously folded autoinhibitory domain. Oncogenic mutations or tyrosine phosphorylation within the

* Corresponding author. Mailing address: Division of Experimental Therapeutics, Ontario Cancer Institute, Princess Margaret Hospital, 610 University Ave., Toronto, Ontario M5G 2M9, Canada. Phone: (416) 946-2233. Fax: (416) 946-2984. E-mail: rottapel@uhnres.utoronto.ca.

† Present address: Glaxo-IMCB Group, Institute of Molecular and Cell Biology, Singapore 117609, Singapore.

Kit JM domain disrupt the autoinhibitory function of this region.

## MATERIALS AND METHODS

**Synthesis and purification of peptides.** Peptides corresponding to murine Kit JM and the kinase insert regions were made by solid-phase synthesis by using standard Fmoc [*N*-(9-fluorenyl)methoxycarbonyl] chemistry on a peptide synthesizer (9050 Plus Pepsynthesizer; PerSeptive Biosystems) and by using PAL-PEG-PS resin (PerSeptive Biosystems). Biotinylation of peptides was achieved by first appending a glycine residue at the amino terminus that acted as a flexible linker and then coupling D-biotin onto the α-amino group of glycine by active-ester reaction. Peptides were cleaved from resin by using 81:13:1:5 (vol/vol) trifluoroacetic acid:thioanisole:anisole:ethanedithiol for 30 min at 25°C. The peptides were precipitated and washed in cold ether and were dissolved in water. Peptides were purified by gel filtration by using Sephadex G-10 followed by reverse-phase high-pressure liquid chromatography (Waters 510 HPLC system; Millipore) with a gradient of 5 to 50% acetonitrile. Peptides were purified to greater than 99% purity, as estimated by matrix-assisted laser desorption ionization time-of-flight mass spectrometry and reverse-phase high-pressure liquid chromatography. Peptide concentrations were measured by absorbance at 280 nm by using the extinction coefficient of tryptophan or tyrosine and was confirmed independently by the Bradford method by using the Coomassie protein assay reagent (Bio-Rad). Other peptides used as kinase substrates were purchased (Sigma Chemicals).

**CD measurements of peptides.** Circular dichroism (CD) spectra were recorded on an Aviv Circular Dichroism Spectrometer model 62DS at 4°C in a 1-mm quartz cuvette. Spectra were obtained from 198 to 260 nm (1 nm bandwidth) on samples containing 100 μM peptide in four different buffers at pH 7.4: (i) 20 mM Tris-Cl; (ii) 20 mM Tris-Cl, 4 M guanidine; (iii) 20 mM sodium phosphate; and (iv) 20 mM sodium phosphate, 10% glycerol. Thermal denaturation measurements were made by monitoring CD of 100 μM peptides in 20 mM Tris-Cl, pH 7.4, at 220 nm over the temperature range of 0 to 100°C.

**GST fusion proteins.** Constructs corresponding to four different portions of the Kit intracellular region were made: (i) the amino-terminal lobe of the kinase domain involved in ATP coordination (residues 583 to 685); (ii) the kinase insert region between the two lobes of the kinase domain (residues 685 to 761); (iii) the carboxy-terminal lobe of the kinase involved in peptide recognition (residues 762 to 927); (iv) the carboxy tail of the intracellular region that follows the kinase domain (residues 928 to 975). The constructs were made by using domain boundaries identified through sequence alignment of class III RTKs (35). cDNAs corresponding to the different portions of Kit were amplified from full-length Kit and were inserted into pGEX-4T vector (Amersham Pharmacia Biotech). Proteins were expressed in the *Escherichia coli* strain BL21(DE3)pLYS-S (Novagen). The glutathione-*S*-transferase (GST) fusion construct of *Yersinia* phosphatase catalytic domain (GST-YOP) was provided by W. T. Miller. Protein induction and purification of GST fusion proteins were carried out as previously described (40).

**Binding assays.** Biotinylated JM peptides were immobilized on streptavidin beads (2.05 mg of peptide per ml of beads) and used to bind either the dephosphorylated JM-deleted form of intracellular Kit (0.9 μM) or the GST fusion proteins of Kit (0.4 mg/ml) in phosphate-buffered saline with 0.1% Triton X-100 (PBS-T). After being rocked at 4°C overnight, beads were washed five times with PBS-T and were boiled in sodium dodecyl sulfate (SDS) sample buffer to elute bound protein. Proteins were resolved by SDS-polyacrylamide gel electrophoresis (PAGE) and were detected by silver staining or immunoblotting after being transferred onto polyvinylidene difluoride membranes.

**Analytical gel filtration of Kit kinase and juxtamembrane peptide complexes.** The JM-deleted form of intracellular Kit protein (final concentration of 4 μM) and JM or aprotinin control peptides (final concentration of 100 μM) were mixed in 10 mM Tris-Cl, pH 8.0, for 1 h at room temperature, spun down, and run on a Sephadex 200 analytical column fitted on a microbore chromatography system (Pharmacia SMART system) preequilibrated in a solution containing 10 mM Tris-Cl (pH 8.0), 50 mM NaCl at a flow rate of 100 μl/min. The presence of protein was monitored at 280 nm. Elution profiles were calibrated with protein molecular size markers. For analyses of gel filtration fractions, the relevant fractions were spotted onto 96-well enzyme-linked immunosorbent assay plates and were probed with α-histidine antibody or avidin-horseradish peroxidase prior to film exposure.

**c-Kit baculoviral constructs.** Constructs of intracellular murine c-Kit kinases were made by using the pFastBacHT baculoviral plasmid vector (Invitrogen Life Technologies). Wild-type Kit kinase (residues 544 to 975) and the JM deletion mutant kinase (residues 587 to 975) were made by using PCR primers corresponding to the appropriate codons. Primers were made with 5′ *Bam*HI and 3′ *Hin*dIII sites for insertion into the baculoviral vector. The following Kit mutants were made by site-directed mutagenesis of wild-type intracellular Kit by using the QuickChange mutagenesis kit (Stratagene) and complementary PCR primers. The ΔVV-JM mutant has residues 558 and 559 deleted, the ΔYV-JM mutant has residues 567 and 568 deleted, and the catalytic domain mutant has a D-to-A substitution at residue 790 in the conserved kinase catalytic loop. Constructs were made with an amino-terminal hexahistidine tag (present in the baculoviral plasmid vector) to facilitate protein purification and were sequenced to verify the absence of copy errors.

**Expression and purification of c-Kit kinases.** Transfection and amplification of Kit baculoviruses were done in *Spodoptera frugiperda* 9 (Sf9) cells according to the manufacturer's protocols (Invitrogen Life Technologies). Approximately 100 ml of baculoviral stock containing $2 \times 10^7$ PFU per ml was produced for each Kit construct. Five-hundred milliliters of Sf9 cells at a density of $10^6$ cells/ml was infected with the baculoviral stock at a multiplicity of infection of 10. For each Kit protein cells were harvested at day 3, which was previously determined to be the peak of protein expression. After centrifugation, the cell pellet was resuspended in 10 ml of cold lysis buffer consisting of 50 mM HEPES (pH 8.0), 300 mM NaCl, 10 mM imidazole, 1% Nonidet P-40, 1 μM phenylmethylsulfonyl fluoride (PMSF), and aprotinin and leupeptin at 10 μg/ml. The lysate was sonicated for 1 min on ice, and all subsequent purification steps proceeded at 4°C. The lysate was centrifuged at 10,000 × *g* for 30 min, and the supernatant was added to 0.5 ml of nickel-nitrilotriacetic acid-agarose (Ni-NTA; Qiagen) previously equilibrated in lysis buffer. Binding of histidine-tagged proteins to the nickel beads was performed by rocking for 30 min. The lysate and resin was poured into a column, and the unbound material was washed off with 50 ml of wash buffer (50 mM HEPES [pH 8.0], 300 mM NaCl, 20 mM imidazole, 1 μM PMSF, and aprotinin and leupeptin at 10 μg/ml). The column was attached to a fraction collector, and bound protein was eluted in 0.4-ml fractions in elution buffer (50 mM HEPES [pH 8.0], 300 mM NaCl, 250 mM imidazole, 1 μM PMSF, and aprotinin and leupeptin at 10 μg/ml). Eluted fractions were analyzed by SDS-PAGE and by Western blotting with α-histidine antibody. Fractions containing recombinant Kit were pooled, and dithiothreitol was added to a concentration of 0.1 mM. Protein was concentrated by ultrafiltration in a Microsep centrifugal device with a molecular size cutoff of 10 kDa (Pall Gelman Laboratory). The protein stock was stored in 40% (vol/vol) glycerol at −20°C. Protein concentration was determined by the Bradford method by using the Coomassie protein assay reagent (Bio-Rad), and purity was assessed by densitometry of duplicate gels by using ImageQuant 4.2 (Molecular Dynamics). The typical yield of recombinant protein was 0.5 mg per liter of culture.

**Dephosphorylation of c-Kit kinases.** For autophosphorylation studies, purified Kit kinases were dephosphorylated by using GST-YOP immobilized on glutathione beads. The kinases were dissolved in phosphatase buffer (50 mM HEPES [pH 7.4], 100 mM NaCl, 0.5 mM EDTA, 5 mM dithiothreitol, 0.01% Triton X-100), added to GST-YOP beads, and rocked overnight at 4°C. Overnight exposures of α-phosphotyrosine Western blots showed complete absence of phosphotyrosine in the dephosphorylated kinases (data not shown).

**Kinase assays.** Phosphorylation of peptide substrates by Kit kinases was measured by using a continuous coupled-kinase assay (1). The assay was initially validated by comparison with the radioactive phosphocellulose-binding assay (6) by using recombinant protein kinase A (New England Biolabs) and Kemptide as the substrate. For the coupled-kinase reaction mixtures, the final mixture contained 100 mM HEPES (pH 7.4), 10 mM $MgCl_2$, 0.1 mM dithiothreitol, 1 mM $Na_3VO_4$, 1 mM phosphoenolpyruvate, 0.5 mM ATP, 0.28 mM NADH, 8 U of pyruvate kinase–12 U of lactate dehydrogenase, 0.1 mM peptide substrate, and 0.3 μM Kit kinase in a 200-μl volume. All reactions were performed in duplicate. Oxidation of NADH was measured spectrophotometrically at 340 nm, 30°C, in a plate reader (Optimax plate reader; Molecular Devices) controlled by automation software (SoftProMax; Molecular Devices). Phosphorylation velocities were calculated from the linear region of the slope of the kinetic curves. $K_m$ ATP measurements were carried out as previously described (7). Velocities were fitted into the Michaelis-Menten equation, and the kinetic parameters $V_{max}$ and $K_m$ were determined by nonlinear regression analysis by using the program MacCurveFit v1.5. For kinase autophosphorylation studies, activity was directly measured in a reaction mixture containing 50 mM HEPES (pH 7.4), 100 mM $MgCl_2$, 4 mM $Na_3VO_4$, 0.5 mM ATP, 0.1 mg of denatured enolase/ml, and concentrations of Kit kinase ranging from 20 to 120 nM. The reaction was initiated by the addition of the kinase and was stopped at each time point by removing a portion of the reaction mixture and rapidly mixing it with SDS sample buffer. Tyrosine phosphorylation was analyzed by SDS-PAGE followed by Western blotting with α-phosphotyrosine antibody. Exposure time for α-phosphotyrosine blots was standardized at 5 min. No significant differences were observed in the phosphor-

ylation profiles of 5- and 30-min exposure times for the α-phosphotyrosine blots. Phosphorylation progress curves were generated by densitometry scanning of Western blots (ImageQuant 4.2) and fitting the phosphorylation values in densitometric units as a function of time into the double-exponential function $F(t) = a \cdot \exp(-b \cdot t) + c \cdot \exp(-d \cdot t) + e$, where $t$ is time and $a$, $b$, $c$, $d$, and $e$ are variables. This was according to a two-stage cooperative activation model for Kit autophosphorylation following the reaction scheme $E_0 + \text{ATP} \xrightarrow{\text{slow}} E_1P + \text{ATP} \xrightarrow{\text{fast}} E_1P_n$, where $E_0$ represents downregulated, dephosphorylated kinase, $E_1P$ represents activated kinase, and $E_1P_n$ represents activated kinase with autophosphorylated sites at saturation.

**JM peptide inhibition of Kit kinase.** The JM peptides were preincubated with wild-type recombinant Kit at various concentrations for 10 min prior to initiation of kinase reactions. For analyses of autophosphorylation inhibition, the same conditions for the autophosphorylation reaction described above were used, except that bovine serum albumin (BSA) was substituted for enolase. The final concentration of Kit kinase was 120 nM, and the concentrations of JM peptides varied from 10 to 60 μM. The peptide aprotinin (66 residues) was used as a specificity control at 120 μM. As the phosphopeptide was largely insoluble in water, dimethyl sulfoxide (DMSO) was used. DMSO was added to the kinase reaction mixture for control and did not affect kinase activity. For analyses of inhibition of exogenous peptide substrate, the radioactive phosphocellulose-binding assay (6) was used. Kit was preactivated by incubating the kinase in buffer containing 100 mM $MgCl_2$ and 1 mM cold ATP for 30 min at room temperature. The JM peptides were then added at various concentrations and were incubated for another 10 min. The reaction was initiated upon addition of radiolabeled ATP and peptide substrate and was performed at room temperature. The final reaction mixture contained 50 mM HEPES (pH 7.4), 100 mM $MgCl_2$, 4 mM $Na_3VO_4$, 0.25 mM ATP, 1/100 volume of [$\gamma$-$^{32}$P]ATP, 1 mg of BSA/ml, 1 mM dynorphin A peptide substrate, 120 nM Kit kinase, and JM peptide at concentrations ranging from 0.1 to 0.6 mM. For examining the role of phosphopeptide in the inhibition of exogenous substrate phosphorylation the conditions for the autophosphorylation reaction described above were used, with 0.1 mg of myelin basic protein/ml.

**Cell culture and proliferation assays.** Rat 2 cells were infected with phoenix E (G. Nolan, Stanford University) retroviral supernatants derived from the pBMN Lyt2 (vector control; G. Nolan, Stanford University) or pBMN Lyt2 Kit Δ27 constructs. Cells were sorted to exclude the uninfected population. Cells infected with pBMN Lyt2 were sorted by using an anti-CD8 α-fluorescein isothiocyanate (FITC)-conjugated antibody, and cells infected with pBMN Lyt2 Kit Δ27 were sorted with an anti-Kit FITC-conjugated monoclonal antibody (Ack2). Vector control and Kit Δ27 Rat 2 cells were transfected with a pcDNA 3.1-based expression vector (Invitrogen) expressing the Kit JM domain fused to green fluorescent protein (GFP) at its carboxy terminus or to GFP alone. Transfected cells were selected by using 0.5 mg of G418/ml in Dulbecco's modified Eagle medium H21 (Invitrogen) containing 10% fetal bovine serum (Cansera) and $5 \times 10^{-5}$ M β-2-mercaptoethanol. Selected cells were counted and plated in triplicate in 48-well culture dishes at a concentration of 2,500 cells/well. At the indicated time points the cells were trypsinized and counted. Growth inhibition of Rat 2 vector control cells and Rat 2 Kit Δ27 cells by the JM domain-GFP fusion protein was expressed as percent inhibition compared to that of cells expressing GFP alone.

## RESULTS

**The JM region contains secondary structure characteristics of a folded domain.** To assess the structural basis of GIST activating mutations in the Kit JM (JM) region, a 38-residue peptide corresponding to the region between the membrane insertion site and the boundary of the N-terminal lobe of the kinase domain was synthesized (GPMYEVQWKVVEEING NNYVYIDPTQLPYDHKWEFPRN). The JM peptide at 100 μM concentration in 20 mM Tris-Cl (pH 7.4) showed a CD spectra suggestive of an ordered state (Fig. 1A). Similar results were obtained for the JM peptide in 20 mM sodium phosphate with or without 10% glycerol. The secondary structure determined by CD spectroscopy was lost in the presence of 4 M guanidine, indicating the transition to an unstructured random coil. To determine the effect of oncogenic mutations on the biophysical properties of the JM region, a 36-residue peptide (ΔVV mutant: GPMYEVQWKEEINGNNYVYIDPTQLPY DHKWEFPRN) corresponding to a human GIST mutation with a two-residue deletion at positions 558 to 559 was synthesized. CD spectra suggested diminished secondary structure of the mutant peptide compared to that of the wild-type peptide and the loss of its residual structure in the presence of 4 M guanidine (Fig. 1B and data not shown).

Following ligand binding, Kit becomes phosphorylated at two neighboring tyrosine residues, $Tyr^{567}$ and $Tyr^{569}$, in the JM region which become docking sites for downstream SH2-containing signaling molecules (24). To examine whether phosphorylation modulated the secondary structure of the Kit JM region, we synthesized a diphosphorylated form of the Kit JM peptide and examined its spectroscopic properties. As shown in Fig. 1B, tyrosine phosphorylation of the Kit JM peptide disrupted all secondary structure, resulting in a completely unfolded coil-coiled conformation.

We next examined the thermal stability of the wild-type JM peptide by taking CD measurements at 220 nm in the temperature range of 0 to 100°C. The peptide showed cooperative temperature-dependent unfolding, a characteristic of an autonomously folded domain (Fig. 1C), with a sharp melting temperature of the folded state at 39°C (Fig. 1D). In distinction from the wild-type JM peptide, neither the tyrosine-phosphorylated peptide (Fig. 1C) nor the oncogenic form (data not shown) exhibited cooperative thermal unfolding indicating the lack of stable secondary structure.

**The JM domain binds to the amino-terminal lobe of the kinase domain.** Repression of kinase activity can occur through interaction between the catalytic domain and other regions of the protein as exemplified by Src family kinases (39, 42). We examined whether the Kit JM interacts with the dephosphorylated intracellular Kit (KitΔjux) catalytic domain. Biotinylated wild-type, mutant, or phosphorylated JM peptides were immobilized on streptavidin beads and were mixed with recombinant KitΔjux His-tagged protein. Bound KitΔjux was then eluted from the beads and was measured semiquantitatively by Western blot analysis by using antihistidine antibodies. The wild-type peptide bound KitΔjux with the highest affinity, while the phosphopeptide had the lowest affinity for the kinase (Fig. 2A). There was no background interaction between the KitΔjux kinase and control beads (Fig. 2A, last lane). To delineate the region of interaction, portions of intracellular Kit were expressed as soluble GST Kit fusion proteins and were analyzed for their capacity to bind to wild-type JM peptide immobilized on beads. JM-GST protein complexes were resolved by SDS gel electrophoresis and were detected by silver staining. We found that the JM peptide bound only to the amino-terminal lobe of the Kit kinase domain (Fig. 2B). The interaction between the wild-type JM peptide and the amino-terminal lobe was dose dependent and was of consistently greater affinity than the mutant peptide (Fig. 2C). Analytical gel filtration was used to examine whether the KitΔjux:JM peptide complex formed in solution. The elution profile of the recombinant KitΔjux protein showed a single monomeric peak corresponding to a molecular size of 53 kDa. Gel filtration of the soluble KitΔjux kinase-JM peptide mixture revealed a higher-molecular-size species demonstrating complex formation of the JM peptide with the catalytic core se-

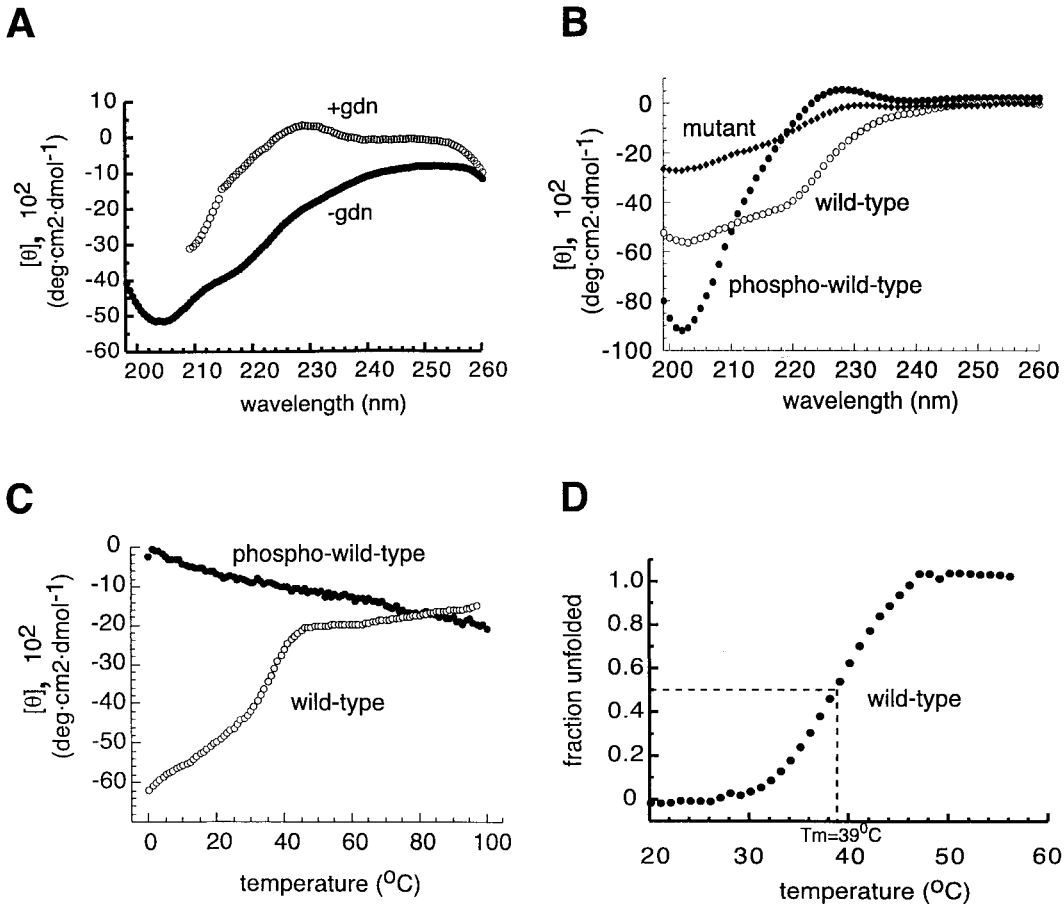


FIG. 1. CD analyses of wild-type, mutant, and diphosphorylated forms of Kit JM peptide. (A) CD spectra of 100 μM wild-type peptide (GPMYEVQWKVVEEINGNNYVYIDPTQLPYDHKWEFPRN) in 20 mM Tris-Cl, pH 7.4 (−gdn), or in 20 mM Tris-Cl, 4 M guanidine, pH 7.4 (+gdn), at 4°C. Similar results were obtained in other aqueous buffers. deg, degrees. (B) Direct comparison of the CD spectra of wild-type, mutant (GPMYEVQWKEEINGNNYVYIDPTQLPYDHKWEFPRN), and diphosphorylated (GPMYEVQWKVVEEINGNNpYVpYIDPT QLPYDHKWEFPRN) forms of Kit JM peptides (all 100 μM in 20 mM Tris-Cl, pH 7.4). (C) Thermal denaturation of wild-type or phospho-wild-type Kit JM peptides (CD measurement at 220 nm). (D) Calculation of the unfolded fraction of the wild-type Kit JM peptide as a function of temperature. The melting temperature ($T_m$) was calculated to be 39°C.

quence of the Kit kinase domain in solution (Fig. 2D, upper panel). The Kit kinase did not bind the control peptide aprotinin. We performed Western blot of the gel filtration fractions to verify that the Kit JM peptide could form a stable complex with KitΔjux kinase in solution (Fig. 2D, lower panel).

**Wild-type and ΔJM mutant Kit kinases exhibit similar specificities toward peptide substrates.** Changes in the substrate specificity of the catalytic domain of protein tyrosine kinases can contribute to transforming potential, as reported for the Ret RTK (36). We generated recombinant forms of wild-type or mutant forms of Kit kinase proteins to evaluate their biochemical properties. All forms were catalytically active, except for Kit D790A, which harbors an inactivating mutation in the kinase domain (Fig. 3). To examine whether mutations in the JM region affected Kit substrate specificity, five synthetic peptides were analyzed as substrates against wild-type and KitΔjux kinases (Fig. 4A): (i) RR-SRC, RRLIE DAEYAARG; (ii) angiotensin I, DRVYIHPFHL; (iii) dynorphin A, YGGFLRRI; (iv) RR-gastrin, RRLEEEEEAYG; and (v) Kit Y719, GSSNEYMDMKPG, a peptide based on the autophosphorylation site in the Kit kinase insert region where the SH2 domain of the p85 subunit of phosphatidyinositol-3-kinase binds (23, 38). The phosphorylation rates of wild-type and KitΔjux kinases were compared by using a coupled-kinase assay (1). No kinetic differences were observed between the two forms of the Kit kinase against these five substrates. Surprisingly, the Y719 peptide was not preferred over the other peptides as a substrate. High effective concentrations of Kit receptor resulting from ligand-induced dimerization may obviate the need for preferential selection of autophosphorylation sites in the kinase insert.

**Wild-type and ΔJM Kit kinases have similar $K_m$ values for ATP.** Allosteric distortion of the ATP binding site resulting from the interaction between the JM and the N-terminal lobe may alter the $K_m$ ATP of the Kit kinase. To examine this possibility, $K_m$ ATP values were measured for the wild-type, KitΔjux, and KitΔYVjux kinases (with residues 567 and 568 deleted in the JM) (Fig. 4B). ATP concentration was varied from 20 to 1,000 μM, and angiotensin I peptide substrate concentration was fixed at 0.5 mM. $K_m$ ATP values for wild-

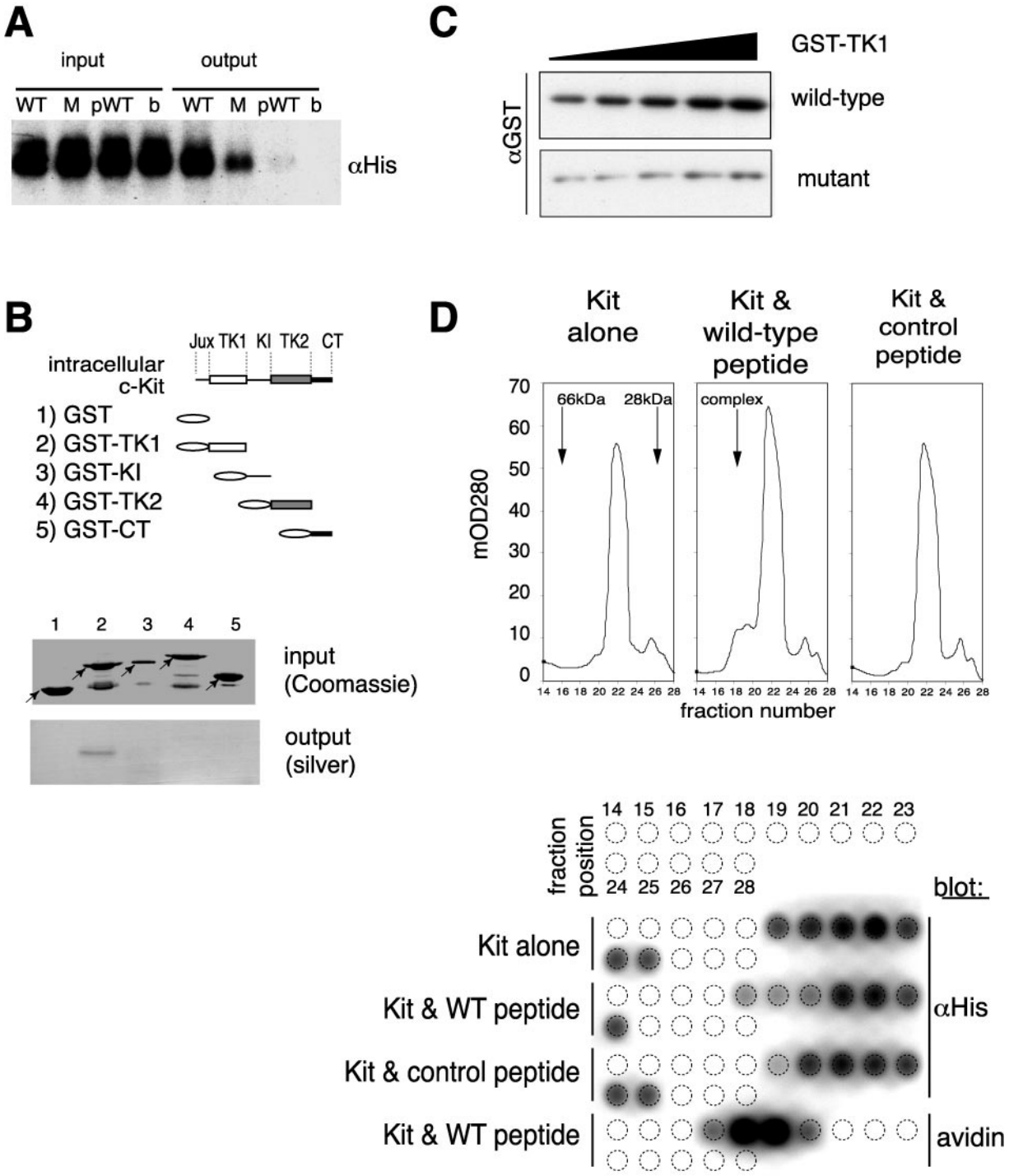


FIG. 2. Binding analyses of wild-type, mutant, and phosphorylated forms of the Kit JM peptide. (A) Differential affinities of wild-type (WT), mutant (M), and phosphorylated (pWT) peptides for intracellular Kit (KitΔjux). The amount of Kit bound to immobilized peptides or to BSA-blocked streptavidin beads (lane b) was detected by α-histidine blotting (output). One out of 20 of the input kinases was loaded for comparison. (B) Mapping of the JM-catalytic domain interaction to the N-terminal kinase lobe. The top portion is a list of GST-Kit fusion proteins made, and the bottom portion is an analysis of GST-Kit fusion proteins (0.4 mg/ml) binding to immobilized wild-type JM peptides as detected by silver staining. Lane numbers correspond to the GST construct assigned above. Arrows point to the relevant protein band. (C) Wild-type and mutant peptides were directly compared in binding to GST-TK1 (increasing concentrations of 22, 27.5, 36.7, 55, and 110 μg/ml) by α-GST blotting. (D) The top portion shows gel filtration of intracellular Kit kinase alone, kinase with wild-type JM peptide, and kinase with control aprotinin peptide. Molecular size standards are indicated in the first graph. The shoulder peak in the middle graph represents the kinase-peptide complex. No complex formation was observed for the aprotinin peptide. The bottom portion shows α-histidine (KitΔjux) and avidin (Kit JM peptide) blotting of gel filtration fractions which demonstrate that the Kit JM forms a stable complex with the entire kinase domain in solution.

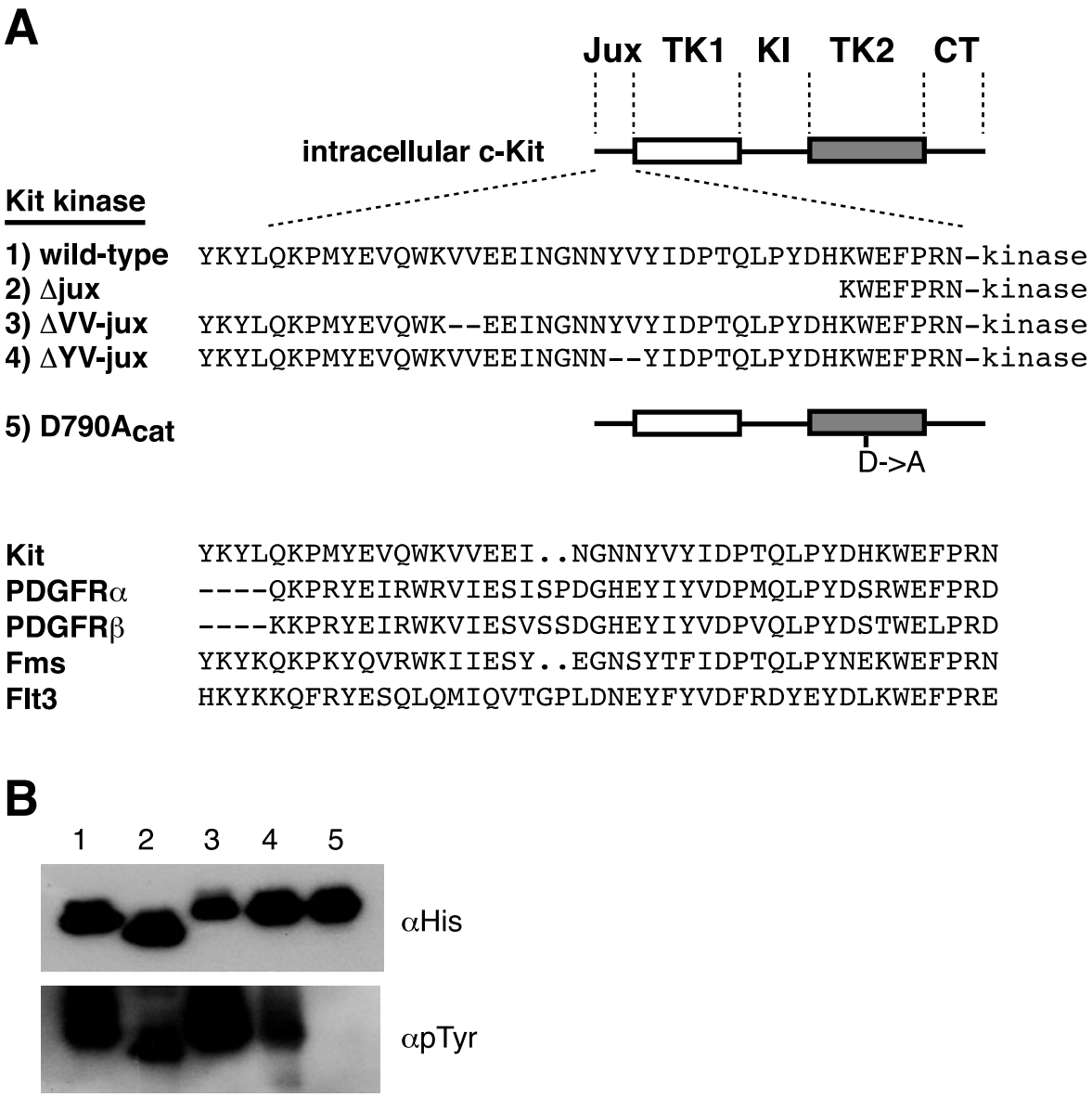


FIG. 3. Expression and activity of recombinant Kit proteins. (A) The top portion shows wild-type, JM mutant, and inactive mutant intracellular Kit kinases expressed by using the baculovirus system. The wild-type kinase comprises the entire intracellular portion. The JM mutant kinases are deletions of the entire JM region, Y544-H579 (Δjux), a double valine ($\Delta V^{558}V^{559}$-jux), or a tyrosine valine ($\Delta Y^{567}V^{568}$-jux). The catalytically inactive D790A mutant carries a mutation in the catalytic loop of the kinase domain. The bottom portion shows sequence alignment of the JM regions of type III RTKs (Kit, PDGFRα and PDGFRβ, Fms, and Flt3). (B) α-Histidine and 4G10 Western blot analyses of Kit kinases. Wild-type and JM mutant Kit kinases were found to be tyrosine phosphorylated after expression and purification, whereas the D790A mutant kinase had no detectable phosphotyrosine. The D790A mutant also exhibited no activity toward exogenous peptide substrates (data not shown). Lane numbers correspond to the Kit kinase assigned in panel A.

type, KitΔjux, and KitΔYVjux kinases were 53.6, 23.0, and 49.1 μM, respectively. Thus, subtle or severe alterations in the Kit JM domain do not appreciably change the binding affinity of ATP to the amino-terminal lobe.

**Mutant Kit kinases have shortened induction times relative to those of wild-type Kit kinase.** Crystal structure determination has shown that the catalytically inactive forms of Src family kinases are stabilized through a series of intramolecular interactions. Kinetic studies that trace the temporal transition of the inactive autoinhibited kinase to the fully activated kinase correlates with the release of these intramolecular interactions. To test whether the intramolecular interaction between the JM and the kinase domains in Kit similarly represses its catalytic activity, the induction times to activation of wild-type and mutant kinases were examined. The rate of autophosphorylation of recombinant dephosphorylated Kit kinase was determined by anti-phosphotyrosine Western blotting as a function of time. Simultaneously, the rate of phosphotransfer to an exogenous substrate was measured. The rate of wild-type Kit phosphorylation showed triphasic sigmoidal kinetics at the lower kinase concentrations of 20 and 40 nM and showed biphasic kinetics at concentrations greater than 80 nM (Fig. 5A). The induction

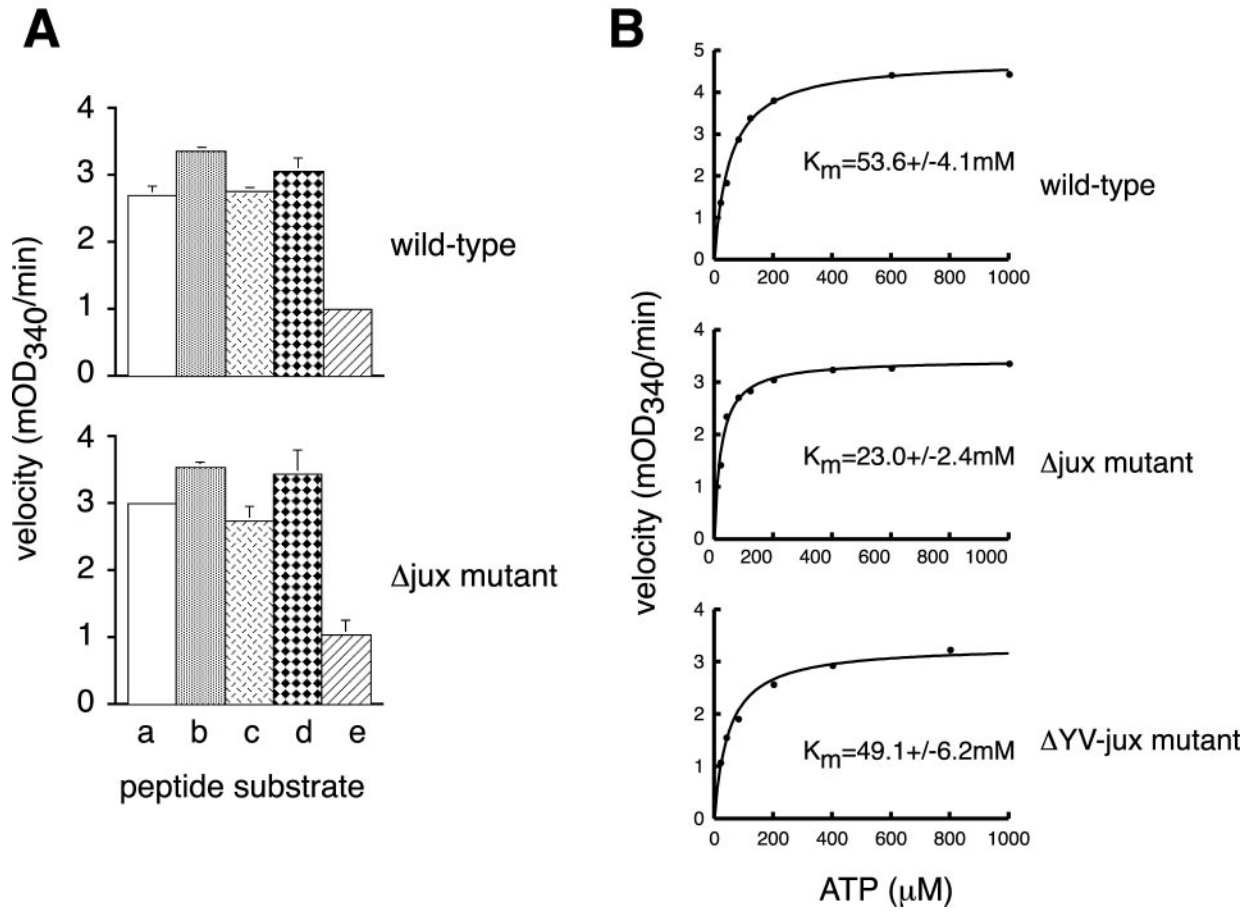


FIG. 4. Exogenous substrate specificities and ATP-binding measurement for wild-type and mutant forms of Kit. (A) The *x* axis corresponds to the peptide substrate as follows: lane a, src-related peptide; lane b, angiotensin I; lane c, dynorphin A; lane d, gastrin; lane e, KitY719. One optical density at 340 nm ($OD_{340}$) unit = 65.2 nmol of NADH. Results represent the mean values of triplicate assays and are presented with standard error bars. The background NADH oxidation rate of 0.12 mOD/min in the absence of kinase was subtracted from the final velocities. (B) $K_m$ ATP was measured for the wild type (0.4 μM), KitΔjux (0.3 μM), and KitΔYVjux (0.3 μM). Spectrophotometric assays of Kit kinases were performed in triplicate by using the peptide substrate angiotensin I with various ATP concentrations. The mean average velocities, after subtracting the background NADH oxidation, were plotted and fitted into the Michaelis-Menten equation, and $K_m$ values were obtained by nonlinear regression analysis.

times to activation were estimated graphically from the intercept of the initial low-velocity phase and the subsequent high-velocity phase. For the kinase at 20, 40, 80, and 120 nM concentrations, the induction times were 3, 2.3, 0.3, and 0.1 min, respectively. The nonlinear relationship between the induction times and kinase concentrations is indicative of a bimolecular transphosphorylation event. We also observed that increasing kinase concentrations resulted in increasing rates of kinase phosphorylation. This is presumably because of a shortened average time between molecular encounters. In the case of a unimolecular *cis* phosphorylation event the kinetics would be expected to be linear and would not be concentration dependent (9).

Progress curves of KitΔjux autophosphorylation showed sharp biphasic curves at all kinase concentrations (Fig. 5B). Induction times for KitΔjux were rapid and occurred within 10 s of initiation of the kinase reaction. Two other Kit mutants bearing two-residue deletions in the JM, KitΔVVjux and KitΔYVjux, were comparable to the KitΔjux mutant in their progress curve profiles (Fig. 5C and D). These results indicate that the JM domain has an inhibitory function in regulating the induction time for maximum kinase activation which is lost in the oncogenic forms of Kit.

**Exogenous JM peptide inhibits Kit kinase activity.** We next tested whether the exogenous JM peptide could directly inhibit Kit activity. Kit autophosphorylation was studied in the presence of wild-type or ΔVV mutant synthetic JM peptides (Fig. 6A). The JM peptides were incubated in various concentrations with the dephosphorylated recombinant wild-type Kit kinase domain for 10 min prior to the addition of MgATP to initiate the reaction. Kit phosphorylation was detected by antiphosphotyrosine immunoblotting. Kit autophosphorylation was inhibited by the wild-type peptide in a dose-dependent manner (Fig. 6A, left panel), whereas the mutant JM peptide demonstrated substantially decreased inhibitory activity (Fig. 6A, right panel, graphically summarized in panel B). The capacity of Kit to autophosphorylate was not affected by the aprotinin control peptide, even at 120 μM (Fig. 6A, right

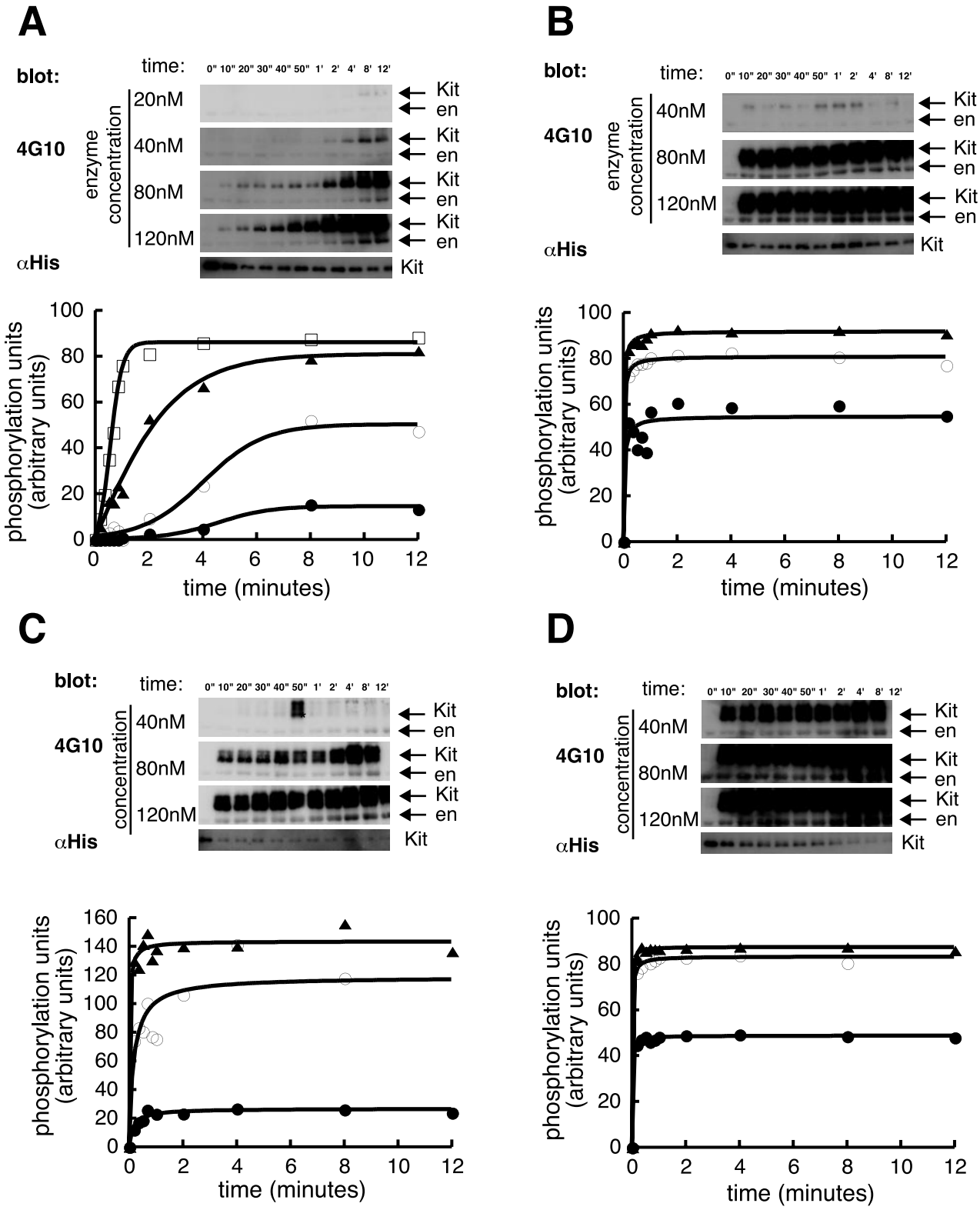


FIG. 5. Activation kinetics of the recombinant dephosphorylated Kit kinase. Autophosphorylation of Kit and phosphorylation of the substrate enolase (en) was analyzed by 4G10 blotting. *y*-axis units were generated by densitometry. These analyses were performed for wild-type (A), Δjux (B), ΔVV-jux (C), and ΔYV-jux (D) kinases. For wild-type Kit, 20, 40, 80, and 120 nM concentrations are represented by filled circles, open circles, filled triangles, and open squares, respectively. For all the mutant kinases, 40, 80, and 120 nM are represented by filled circles, open circles, and filled triangles, respectively. The 50-s time point at the 40 nM kinase concentration (*) of panel C was an outlying value and was not used in generating the progress curve. Results are representative of three independent experiments.

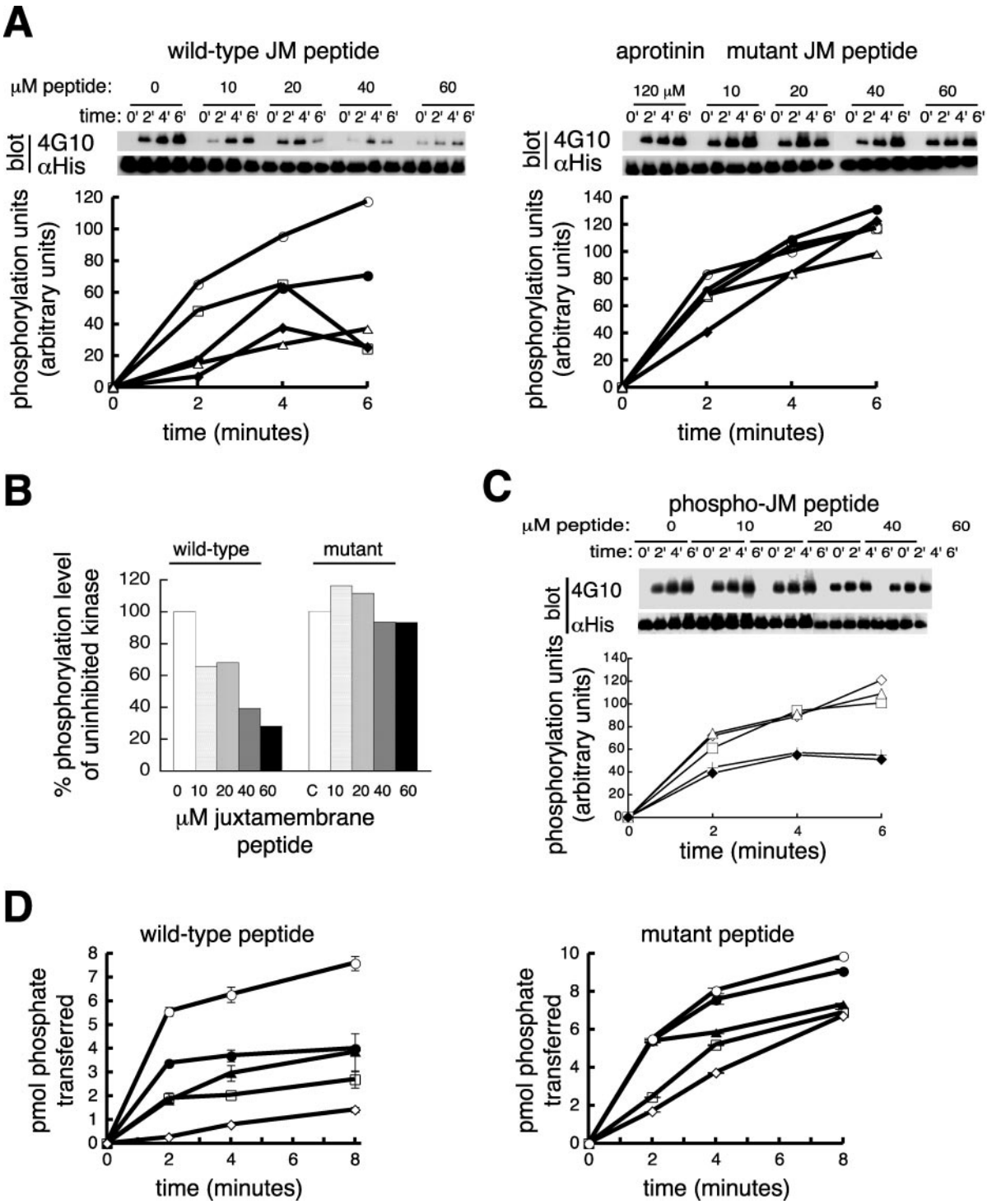


FIG. 6. Inhibition of full-length intracellular Kit kinase activity by JM peptides in *trans*. (A) Inhibition of autophosphorylation. Dephosphorylated recombinant Kit kinase was incubated with various concentrations of wild-type or mutant JM peptide. Kit autophosphorylation was assayed at the indicated time points by 4G10 blotting. No inhibition of Kit kinase activity was observed with the control aprotinin peptide at 120 μM (right panel). Peptide concentrations of 0, 10, 20, 40, and 60 μM are represented by open circles, filled circles, open squares, filled diamonds, and open triangles, respectively. These results are representative of two independent experiments. (B) Percent inhibition is calculated from the phosphorylation units shown in panel A at 4 min. Kit autophosphorylation in the absence of the JM peptide was normalized to 100%. (C) Kit autophosphorylation in the presence of phospho-JM peptide. The conditions used were the same as those described for panel A. Phosphopeptide concentrations of 0, 10, 20, 40, and 60 μM are represented by open squares, open diamonds, open triangles, crosses, and filled diamonds, respectively. (D) In *trans* inhibition of substrate phosphorylation by Kit JM peptides. The phosphorylation of the exogenous peptide substrate dynorphin A (1 mM) by preactivated Kit was measured in the presence of [$\gamma$-$^{32}$P]ATP and JM wild-type and mutant peptides at 0 (open circles), 0.1 (filled circles), 0.2 (filled triangles), 0.4 (open squares), and 0.6 μM (open diamonds) concentrations. $^{32}$P incorporation was converted to picomoles of phosphate. The values are the means of triplicate assays and are presented with standard error bars.

panel). In order to determine if tyrosine phosphorylation of the JM peptide altered its inhibitory activity, we examined Kit kinase autophosphorylation in the presence of the diphosphorylated JM peptide. We observed that in distinction to the unphosphorylated wild-type form of the peptide, the diphosphorylated peptide was similar to the mutant peptide and was largely unable to inhibit Kit autophosphorylation. (Fig. 6C).

To test whether the transition from the repressed state to the activated state of the kinase was reversible and dependent on the concentration of the JM peptide, we next determined if the soluble JM peptide could inhibit the preactivated form of the Kit kinase. Kit was allowed to autophosphorylate for 30 min prior to assaying its capacity to phosphorylate exogenous substrate as a measure of its kinase activity in the presence of the wild-type or mutant JM peptide (Fig. 6D). We found that the wild-type JM peptide inhibited substrate phosphorylation in a dose-dependent manner, whereas the mutant peptide was a less effective inhibitor. Addition of the phosphorylated JM peptide had no inhibitory effect on the capacity of preactivated Kit to phosphorylate exogenous substrates (data not shown). These results show that exogenous wild-type JM can stabilize the repressed form of Kit regardless of its activation state, a function that is significantly reduced when the JM region contains oncogenic mutations or when the Kit JM domain is tyrosine phosphorylated.

**Growth suppression of a Kit-transformed cell line by ectopic expression of the Kit JM domain.** In order to determine if the Kit JM domain could interfere with the oncogenic activity of Kit in living cells, we ectopically expressed a GFP-tagged version of the Kit JM in cells that harbor an oncogenic form of Kit mutated in its JM domain (33). Rat 2 cells were infected with a retrovirus expressing either the CD8 cell surface epitope (pBMN Lyt2) or both CD8 and a constitutively active form of Kit with nine amino acids deleted within its JM domain (pBMN Lyt2; Kit Δ27). Cells were sorted to exclude the uninfected population by using an anti-CD8 α-FITC-conjugated antibody. Kit Δ27-expressing cells were then sorted by using an anti-Kit monoclonal antibody (Ack2). A population of CD8-positive control Rat 2 cells or Kit Δ27 expressing Rat 2 cells were then transfected with an expression vector either for GFP or the Kit JM domain fused to GFP at its carboxy terminus. Transfected cells were selected in G418 and were verified for Kit JM expression by fluorescence microscopy. Known numbers of drug-selected cells were seeded in complete medium, and cell growth was estimated after 40, 60, or 90 h of culture. We observed that the growth of Rat 2 control cells was not affected by the expression of the Kit JM domain. However, the expression of the Kit JM domain in the Kit Δ27 cells resulted in 40 to 60% growth inhibition at all time points (Fig. 7). These data show that the isolated Kit JM domain can not only interfere with the catalytic activity of Kit in vitro but can also specifically suppress Kit-dependent cell growth in vivo.

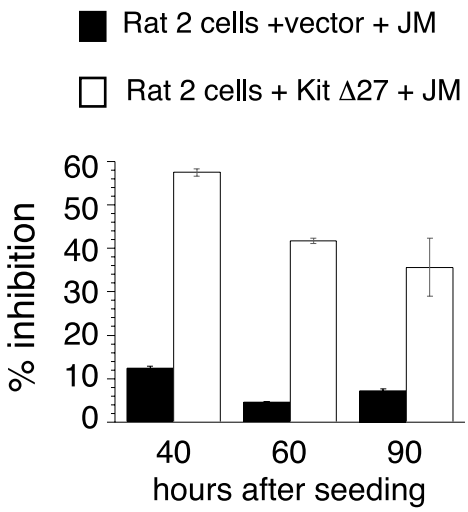


FIG. 7. Growth suppression of a Kit-transformed cell line by ectopic expression of the Kit JM domain. Rat 2 cells expressing either the vector alone (pBMN Lyt2) or a constitutively active form of Kit (pBMN Lyt2; Kit Δ27) were selected by cell sorting. Vector control and Kit Δ27 Rat 2 cells were subsequently transfected with either GFP alone or with the Kit JM domain fused to GFP at its carboxy terminus, selected in G418, and verified for GFP expression by fluorescence microscopy. Known numbers of the selected cells were seeded, and cell growth was estimated after 40, 60, or 90 h of culture. Data shown are percent growth inhibition in cells expressing Kit JM relative to that of GFP-transfected controls.

## DISCUSSION

Protein kinases are commonly regulated by *cis*-acting elements that stabilize a catalytically inactive conformation such that the MgATP, peptide substrates, or catalytic residues are prevented from adopting the correct orientation required for efficient phosphotransfer (16). Well-characterized examples include the insulin receptor and the fibroblast growth factor receptor, whose catalytic active sites are occluded by their activation segments in the carboxy-terminal lobe (17, 30). Examples of protein kinases regulated by *cis*-acting inhibitory elements lying outside of the catalytic domain include the SH3 and SH2 domains of Src family kinases (39, 42), the kinase inhibitory linker of Pak1 (5, 22), and the phosphorylated amino-terminal segment of GSK3β (8, 10).

Here we show that the cytosolic JM region of Kit serves an autoinhibitory function. We have shown the Kit JM behaves as an autonomously folding domain that binds directly to the amino-terminal lobe of the Kit kinase and prolongs its induction time to activation. Strikingly, we have shown that a synthetic form of the Kit JM can act in *trans* to repress the catalytic activity of Kit. We have shown that the tyrosine-phosphorylated form of this peptide exhibits profoundly different properties from those of the wild-type peptide. Namely, phosphorylation results in a drastic change in the secondary structure of the JM domain and interferes with its capacity to bind to the N-terminal lobe of the Kit kinase and is no longer able to repress the catalytic activity of Kit. These data suggest that tyrosine phosphorylation composes the switch that transforms the JM domain from a conformation mediating autoinhibition of the kinase to one consistent with the adoption of a catalytically productive state. The tyrosine-phosphorylated JM may also serve to potentiate the recruitment of downstream SH2-containing signaling molecules to the kinase.

Recombinant forms of Kit in which the JM is either mutated or deleted demonstrate extremely rapid activation kinetics. A mutant JM peptide derived from an oncogenic form of Kit shows disordered secondary structure, decreased binding af-

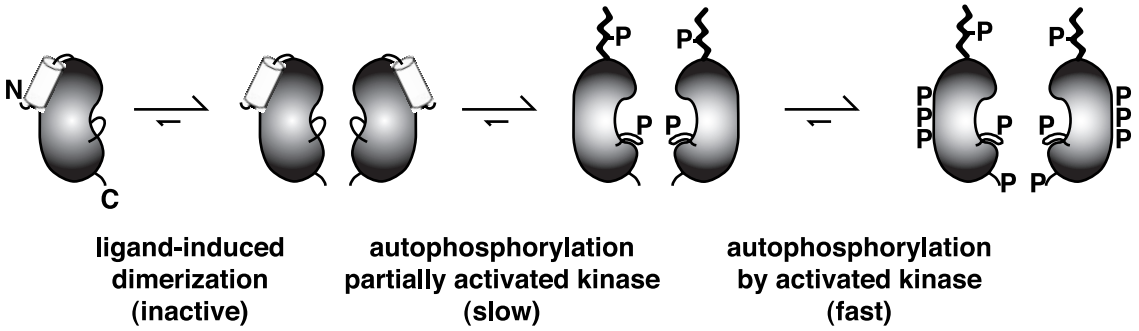


FIG. 8. Model of Kit activation through JM-mediated autoinhibition. The Kit JM domain is portrayed as a cylinder. P represents phosphotyrosine residues. Monomeric Kit is autoinhibited by the interaction of the JM domain with the N-terminal kinase lobe prior to ligand stimulation. Ligand-induced dimerization drives autophosphorylation at the slow rate of the repressed kinase. Activation of Kit involves phosphorylation of the JM domain and activation segment. Once phosphorylated, the JM domain loses its secondary structure and is released from the N-terminal lobe. The kinase then undergoes rapid autophosphorylation characteristic of the fully activated state.

finity to the amino-terminal lobe of the kinase domain, and a diminished capacity to repress Kit catalytic activity. These observations are consistent with genetic data that show the high frequency of mutations in the cytosolic JM region of Kit in human, murine, and canine cancers (26–28). Moreover, mutations in the Kit JM domain that disturb its structure result in ligand-independent kinase activation. Ectopic expression of these JM mutated forms of Kit render hematopoietic cell lines factor independent, demonstrating that these mutant forms of Kit are sufficient for cell transformation (15). The JM domain is highly conserved in other members of the class III RTK family. This suggests that the JM region may play a similar repressive function in these receptors. For example, the gene of Flt3 RTK, the most frequently mutated gene in human acute myeloid leukemia, harbors mutations clustered within its JM region (32). Inhibition of activated Kit in GIST tumors by the ATP-binding antagonist STI571 has demonstrated that Kit is a drug-susceptible target in the clinical setting (20). The in vivo inhibition of an oncogenic version of Kit by the expression of the Kit JM peptide may form the basis of a cell-based strategy to discover new Kit inhibitor molecules. Identification of small-molecule mimetics of the Kit JM could be an approach towards developing novel Kit and related class III RTK inhibitors that are structurally distinct from the conventional kinase active-site inhibitors.

We propose a step-wise model for Kit activation, shown in Fig. 8. In the absence of its ligand, monomeric Kit receptor is autoinhibited through intramolecular interactions between the JM and its amino-terminal kinase lobe. Ligand-induced dimerization results in high effective concentrations of the kinase domain poised for transphosphorylation at the slow rate of the repressed kinase. Activation of Kit involves phosphorylation of the JM domain and the activation segment. Once phosphorylated, the JM domain loses its secondary structure and is released from the N-terminal lobe. This allows rearrangement and phosphorylation of residues in the catalytic structure, including the activation loop. The kinase then undergoes rapid autophosphorylation characteristic of the fully activated state. Phosphorylation of the Kit JM domain may also allow this region to couple to SH2-containing signaling molecules, such as Lyn (25), Shp1 (21), and Chk (34), or mediate internalization, as has been reported for Fms (31).

Binding of the JM region to the amino-terminal lobe of receptor protein kinases may be a general strategy by which these proteins are autoinhibited, as has been demonstrated by the structural studies of transforming growth factor β receptor (18) and Eph B2 (41). It is important to bear in mind that the primary sequence of the JM regions of these three receptors are quite different and suggest that there may be critical differences in the manner in which the JM regions operate as regulatory switches in these receptors. Detailed understanding of the mechanism underlying the autoinhibitory properties of the Kit JM domain awaits solution of the three-dimensional structure of the entire Kit intracellular region.

## ACKNOWLEDGMENTS

We thank S. Go, Z. Li from Frank Sicheri's lab, and J. Yong (Glaxo-IMCB) for technical assistance. W. Todd Miller kindly provided the GST-YOP construct. We also thank Frank Sicheri and Julie Forman-Kay for helpful comments on the manuscript.

R.R. is a Canadian Institutes of Health Research scientist. This work was supported by an operating grant from the Terry Fox foundation of the NCIC.

## REFERENCES

1. **Barker, S. C., D. B. Kassel, D. Weigl, X. Huang, M. A. Luther, and W. B. Knight.** 1995. Characterization of pp60c-src tyrosine kinase activities using a continuous assay: autoactivation of the enzyme is an intermolecular autophosphorylation process. Biochemistry **34:**14843–14851.
2. **Baxter, R. M., J. P. Secrist, R. R. Vaillancourt, and A. Kazlauskas.** 1998. Full activation of the platelet-derived growth factor beta-receptor kinase involves multiple events. J. Biol. Chem. **273:**17050–17055.
3. **Besmer, P., J. E. Murphy, P. C. George, F. H. Qiu, P. J. Bergold, L. Lederman, H. W. Snyder, Jr., D. Brodeur, E. E. Zuckerman, and W. D. Hardy.** 1986. A new acute transforming feline retrovirus and relationship of its oncogene v-kit with the protein kinase gene family. Nature **320:**415–421.
4. **Binns, K. L., P. P. Taylor, F. Sicheri, T. Pawson, and S. J. Holland.** 2000. Phosphorylation of tyrosine residues in the kinase domain and juxtamembrane region regulates the biological and catalytic activities of Eph receptors. Mol. Cell. Biol. **20:**4791–4805.
5. **Buchwald, G., E. Hostinova, M. G. Rudolph, A. Kraemer, A. Sickmann, H. E. Meyer, K. Scheffzek, and A. Wittinghofer.** 2001. Conformational switch and role of phosphorylation in PAK activation. Mol. Cell. Biol. **21:**5179–5189.
6. **Casnellie, J. E.** 1991. Assay of protein kinases using peptides with basic residues for phosphocellulose binding. Methods Enzymol. **200:**115–120.
7. **Chan, P. M., H. P. Nestler, and W. T. Miller.** 2000. Investigating the substrate specificity of the HER2/Neu tyrosine kinase using peptide libraries. Cancer Lett. **160:**159–169.
8. **Dajani, R., E. Fraser, S. M. Roe, N. Young, V. Good, T. C. Dale, and L. H. Pearl.** 2001. Crystal structure of glycogen synthase kinase 3 beta: structural basis for phosphate-primed substrate specificity and autoinhibition. Cell **105**:721–732.

9. **Fersht, A.** 1985. Enzyme structure and mechanism, 2nd ed. W. H. Freeman and Company, New York, N.Y.
10. **Frame, S., P. Cohen, and R. M. Biondi.** 2001. A common phosphate binding site explains the unique substrate specificity of GSK3 and its inactivation by phosphorylation. Mol. Cell **7:**1321–1327.
11. **Furitsu, T., T. Tsujimura, T. Tono, H. Ikeda, H. Kitayama, U. Koshimizu, H. Sugahara, J. H. Butterfield, L. K. Ashman, Y. Kanayama, et al.** 1993. Identification of mutations in the coding sequence of the proto-oncogene c-kit in a human mast cell leukemia cell line causing ligand-independent activation of c-kit product. J. Clin. Investig. **92:**1736–1744.
12. **Gille, H., J. Kowalski, L. Yu, H. Chen, M. T. Pisabarro, T. Davis-Smyth, and N. Ferrara.** 2000. A repressor sequence in the juxtamembrane domain of Flt-1 (VEGFR-1) constitutively inhibits vascular endothelial growth factor-dependent phosphatidylinositol 3′-kinase activation and endothelial cell migration. EMBO J. **19:**4064–4073.
13. **Hayakawa, F., M. Towatari, H. Kiyoi, M. Tanimoto, T. Kitamura, H. Saito, and T. Naoe.** 2000. Tandem-duplicated Flt3 constitutively activates STAT5 and MAP kinase and introduces autonomous cell growth in IL-3-dependent cell lines. Oncogene **19:**624–631.
14. **Heldin, C. H.** 1995. Dimerization of cell surface receptors in signal transduction. Cell **80:**213–223.
15. **Hirota, S., K. Isozaki, Y. Moriyama, K. Hashimoto, T. Nishida, S. Ishiguro, K. Kawano, M. Hanada, A. Kurata, M. Takeda, G. Muhammad Tunio, Y. Matsuzawa, Y. Kanakura, Y. Shinomura, and Y. Kitamura.** 1998. Gain-of-function mutations of c-kit in human gastrointestinal stromal tumors. Science **279:**577–580.
16. **Hubbard, S. R.** 2002. Autoinhibitory mechanisms in receptor tyrosine kinases. Front. Biosci. **7:**d330–d340.
17. **Hubbard, S. R., L. Wei, L. Ellis, and W. A. Hendrickson.** 1994. Crystal structure of the tyrosine kinase domain of the human insulin receptor. Nature **372:**746–754.
18. **Huse, M., Y. G. Chen, J. Massague, and J. Kuriyan.** 1999. Crystal structure of the cytoplasmic domain of the type I TGF beta receptor in complex with FKBP12. Cell **96:**425–436.
19. **Irusta, P. M., and D. DiMaio.** 1998. A single amino acid substitution in a WW-like domain of diverse members of the PDGF receptor subfamily of tyrosine kinases causes constitutive receptor activation. EMBO J. **17:**6912–6923.
20. **Joensuu, H., P. J. Roberts, M. Sarlomo-Rikala, L. C. Andersson, P. Tervahartiala, D. Tuveson, S. Silberman, R. Capdeville, S. Dimitrijevic, B. Druker, and G. D. Demetri.** 2001. Effect of the tyrosine kinase inhibitor STI571 in a patient with a metastatic gastrointestinal stromal tumor. N. Engl. J. Med. **344:**1052–1056.
21. **Kozlowski, M., L. Larose, F. Lee, D. M. Le, R. Rottapel, and K. A. Siminovitch.** 1998. SHP-1 binds and negatively modulates the c-Kit receptor by interaction with tyrosine 569 in the c-Kit juxtamembrane domain. Mol. Cell. Biol. **18:**2089–2099.
22. **Lei, M., W. Lu, W. Meng, M. C. Parrini, M. J. Eck, B. J. Mayer, and S. C. Harrison.** 2000. Structure of PAK1 in an autoinhibited conformation reveals a multistage activation switch. Cell **102:**387–397.
23. **Lev, S., D. Givol, and Y. Yarden.** 1992. Interkinase domain of kit contains the binding site for phosphatidylinositol 3′ kinase. Proc. Natl. Acad. Sci. USA **89:**678–682.
24. **Linnekin, D.** 1999. Early signaling pathways activated by c-Kit in hematopoietic cells. Int. J. Biochem. Cell Biol. **31:**1053–1074.
25. **Linnekin, D., C. S. DeBerry, and S. Mou.** 1997. Lyn associates with the juxtamembrane region of c-Kit and is activated by stem cell factor in hematopoietic cell lines and normal progenitor cells. J. Biol. Chem. **272:**27450–27455.
26. **Longley, B. J., M. J. Reguera, and Y. Ma.** 2001. Classes of c-KIT activating mutations: proposed mechanisms of action and implications for disease classification and therapy. Leuk. Res. **25:**571–576.
27. **Ma, Y., B. J. Longley, X. Wang, J. L. Blount, K. Langley, and G. H. Caughey.** 1999. Clustering of activating mutations in c-KIT's juxtamembrane coding region in canine mast cell neoplasms. J. Investig. Dermatol. **112:**165–170.
28. **Miettinen, M., and J. Lasota.** 2001. Gastrointestinal stromal tumors–definition, clinical, histological, immunohistochemical, and molecular genetic features and differential diagnosis. Virchows Arch. **438:**1–12.
29. **Mizuki, M., R. Fenski, H. Halfter, I. Matsumura, R. Schmidt, C. Muller, W. Gruning, K. Kratz-Albers, S. Serve, C. Steur, T. Buchner, J. Kienast, Y. Kanakura, W. E. Berdel, and H. Serve.** 2000. Flt3 mutations from patients with acute myeloid leukemia induce transformation of 32D cells mediated by the Ras and STAT5 pathways. Blood **96:**3907–3914.
30. **Mohammadi, M., J. Schlessinger, and S. R. Hubbard.** 1996. Structure of the FGF receptor tyrosine kinase domain reveals a novel autoinhibitory mechanism. Cell **86:**577–587.
31. **Myles, G. M., C. S. Brandt, K. Carlberg, and L. R. Rohrschneider.** 1994. Tyrosine 569 in the c-Fms juxtamembrane domain is essential for kinase activity and macrophage colony-stimulating factor-dependent internalization. Mol. Cell. Biol. **14:**4843–4854.
32. **Nakao, M., S. Yokota, T. Iwai, H. Kaneko, S. Horiike, K. Kashima, Y. Sonoda, T. Fujimoto, and S. Misawa.** 1996. Internal tandem duplication of the flt3 gene found in acute myeloid leukemia. Leukemia **10:**1911–1918.
33. **Plo, I., D. Lautier, N. Casteran, P. Dubreuil, M. Arock, and G. Laurent.** 2001. Kit signaling and negative regulation of daunorubicin-induced apoptosis: role of phospholipase Cγ. Oncogene **20:**6752–6763.
34. **Price, D. J., B. Rivnay, Y. Fu, S. Jiang, S. Avraham, and H. Avraham.** 1997. Direct association of Csk homologous kinase (CHK) with the diphosphorylated site Tyr568/570 of the activated c-KIT in megakaryocytes. J. Biol. Chem. **272:**5915–5920.
35. **Qiu, F. H., P. Ray, K. Brown, P. E. Barker, S. Jhanwar, F. H. Ruddle, and P. Besmer.** 1988. Primary structure of c-kit: relationship with the CSF-1/PDGF receptor kinase family–oncogenic activation of v-kit involves deletion of extracellular domain and C terminus. EMBO J. **7:**1003–1011.
36. **Santoro, M., F. Carlomagno, A. Romano, D. P. Bottaro, N. A. Dathan, M. Grieco, A. Fusco, G. Vecchio, B. Matoskova, M. H. Kraus, et al.** 1995. Activation of RET as a dominant transforming gene by germline mutations of MEN2A and MEN2B. Science **267:**381–383.
37. **Schlessinger, J.** 2000. Cell signaling by receptor tyrosine kinases. Cell **103:**211–225.
38. **Serve, H., Y. C. Hsu, and P. Besmer.** 1994. Tyrosine residue 719 of the c-kit receptor is essential for binding of the P85 subunit of phosphatidylinositol (PI) 3-kinase and for c-kit-associated PI 3-kinase activity in COS-1 cells. J. Biol. Chem. **269:**6026–6030.
39. **Sicheri, F., I. Moarefi, and J. Kuriyan.** 1997. Crystal structure of the Src family tyrosine kinase Hck. Nature **385:**602–609.
40. **Till, J. H., P. M. Chan, and W. T. Miller.** 1999. Engineering the substrate specificity of the Abl tyrosine kinase. J. Biol. Chem. **274:**4995–5003.
41. **Wybenga-Groot, L. E., B. Baskin, S. H. Ong, J. Tong, T. Pawson, and F. Sicheri.** 2001. Structural basis for autoinhibition of the EphB2 receptor tyrosine kinase by the unphosphorylated juxtamembrane region. Cell **106:**745–757.
42. **Xu, W., S. C. Harrison, and M. J. Eck.** 1997. Three-dimensional structure of the tyrosine kinase c-Src. Nature **385:**595–602.